

Improving the Content Uniformity of a Low-Dose Tablet Formulation Through Roller Compaction Optimization

Mary T. am Ende, Sara K. Moses, Anthony J. Carella, Rashmi A. Gadkari,
Timothy W. Graul, Angel L. Otano, and Robert J. Timpano

Pfizer Global Research & Development, Groton, CT

In this investigation, the potency distribution of a low-dose drug in a granulation was optimized through a two-part study using statistically designed experiments. The purpose of this investigation was to minimize the segregation potential by improving content uniformity across the granule particle size distribution, thereby improving content uniformity in the tablet. Initial operating parameters on the Gerteis 3-W-Polygran 250/100/3 Roller Compactor resulted in a U-shaped potency function (potency vs. granule particle size) with superpotent fines and large granules. The roller compaction optimization study was carried out in two parts. Study I used a full factorial design with roll force (RF) and average gap width (GW) as independent variables and Study II used a D-optimal response surface design with four factors: RF, GW, granulating sieve size (SS), and granulator speed (GS). The planned response variables for Study I were bypass weight % and potency of bypass. Response variables for Study II included mean granulation potency with % relative standard deviation (% RSD), granulation particle size, sieve cut potency % RSD, tablet potency with % RSD, compression force at 7 kP crushing strength, and friability of 7-kP tablets. A constraint on GW was determined in Study I by statistical analysis. Bypass and observations of ribbon splitting were minimized when GW was less than 2.6 mm. In Study II, granulation potency, granulation uniformity, and sieve cut uniformity were optimized when the SS was 0.8 mm. Higher RF during dry granulation produced better sieve cut uniformity and tablets with improved uniformity throughout the run, as measured by stratified tablet samples taken during compression and assayed for potency. The recommended optimum roller compaction and milling operating parameters that simultaneously met all constraints were RF = 9 kN, GW = 2.3 mm, SS = 0.8 mm, and GS = 50 rpm. These parameters became the operating parameter set

points during a model confirmation trial. The results from the confirmation trial proved that the new roller compaction and milling conditions reduced the potential for segregation by minimizing the granulation potency variability as a function of particle size as expressed by sieve cut potency % RSD, and thus improved content uniformity of stratified tablet samples.

Keywords roller compaction, dry granulation, segregation, content uniformity, low dose, experimental design

INTRODUCTION

The purpose of this study was to improve drug content uniformity for a low-dose tablet formulation by optimization of the dry granulation process. To that end, an immediate-release tablet containing a model, potent drug candidate was developed with a target potency of 0.5 mg in a 100-mg tablet (< 1% drug loading). The physical and mechanical properties of the blend and granulation for low-dose products is predominantly influenced by the major diluents and not the active ingredient.^[1] Dry granulation may be used to enhance the incorporation of a low-dose drug within each granule to improve potency uniformity and reduce the likelihood of segregation during processing.

The two main particle segregation mechanisms that occur in pharmaceutical powders are sifting and entrainment of air (fluidization).^[2] Sifting occurs when the smaller particles move through the larger particles, as when discharging a blender. This phenomenon results in a high concentration of fines in the center of the powder with the coarser particles rolling to the outer boundaries. Fluidization is caused by the lower permeability of small particles to air, which results in longer retention times for small particles in the air stream. The fluidization segregation mechanism produces a vertical inhomogeneity of the

Received 3 October 2006, Accepted 25 January 2007.

Address correspondence to Mary T. am Ende, Solids Development Group, Oral Products Center of Emphasis, Pfizer Inc., Eastern Point Road (MS 8156-01), Groton, CT 06340; E-mail: Mary.T.am.Ende@pfizer.com

powder in a bin with fines concentrated at the top. Segregation can be detected by monitoring blend and tablet potency uniformity according to the stratified sampling approach reported in the FDA Draft Guidance.^[3]

Segregation of pharmaceutical powders is of most concern during direct compression processing. However, dry granulation for low-dose active ingredients may also pose a risk for segregation. One major reason for this risk is that most roller compactor designs result in a high amount of bypass, or ungranulated material that bypasses the rollers. The proportion of bypass can directly impact granulation uniformity, as measured by granulation particle size, granulation potency % RSD and sieve cut potency % RSD. Bypass may also have an effect on tablet potency uniformity and compaction-bonding properties (e.g., friability and crushing strength from the hardness compression profile). The Gerteis 3-W-Polygran roller compactor was designed with the rolls on a 30° incline to improve the control and ribbon quality.^[4] One major benefit of the Gerteis design is the reduction in bypass from approximately 15–20% to 5–15%. Shlieout et al. discussed the critical process parameters for the Gerteis roller compactor.^[5,6]

The purpose of this study was to determine whether drug uniformity for a low-dose granulated product could be affected by roller compaction and milling processing conditions. This was accomplished by selecting the physical properties of the diluents that accentuated the potential for segregation by using large particle size diluents similar in size (approximately 180 µm) compared to small particle size drug (< 25 µm). The diluents were selected to minimize their relative segregation and to maximize potential for API to segregate, thus enhancing the segregation driving force. This strategy provided an opportunity for the optimized dry granulation conditions to elicit an effect on the granulation content uniformity. An important factor to that may aid to promote uniformity during blending for low-dose, small particle size drug substances is carrier-mediated mixing.^[7] However, this factor affects the blend prior to granulation and therefore our investigation focused on the granulation and tablet uniformity aspects only.

The literature predominates with examples showing the application of roller compaction process optimization to achieve improved performance during subsequent tablet compression, specifically in terms of recompressibility.^[8–14] Alternatively, one group took a novel approach by optimizing roller compaction to improve bioadhesive properties as measured by dissolution, buccal bioadhesion force, and bioadhesion energy.^[15] Von Eggelkraut-Gottanka et al. performed design of experiments to optimize the Gerteis roller compactor to improve not only tableting properties (i.e., sticking and capping) but also product

performance (i.e., disintegration and dissolution).^[16–17] Missing from the literature is research focused on the optimization of drug uniformity within the granulation. In fact, little is known about the effects of the compaction and milling parameters on the content uniformity of a low-dose drug in a tablet formulation. The goal of this investigation was to optimize the roller compaction and milling parameters for a low-dose tablet formulation to produce a uniform distribution of drug in the granulation, and subsequently to improve tablet uniformity.

MATERIALS AND METHODS

Materials

The formulation used for these statistically designed experiments was composed of 0.5 mg of an investigational drug candidate in a 100-mg tablet. The tablet formulation, shown in Table 1, contains two diluents and included microcrystalline cellulose (Avicel PH200®; FMC Corporation, Philadelphia, PA) in which the nominal mean particle size was approximately 180 µm and bulk density of 0.34 g/cm³^[18] and dibasic calcium phosphate anhydrous (A-Tab®; Rhodia Pharmaceutical Ingredients, Cranbury, NJ) in which the nominal mean particle size was 180 µm and bulk density of 0.78.^[18] Colloidal silicon dioxide (Cab-O-Sil®; Cabot Corp., Tuscola, IL) is incorporated as a glidant and croscarmellose sodium (Ac-Di-Sol®; FMC Corporation) as a disintegrant at precedent levels for dry granulated formulations.^[1] The lubricant is vegetable sourced magnesium stearate (Mallinckrodt, Hazelwood, MO). These excipients are commonly used in the field for dry granulation processing.

Table 1
Composition of the 0.5 and 1.0 mg Tablet Formulation for Low Dose Dry Granulation Process Optimization Study

| Component | Weight Percentage (%) | 0.5 mg (mg/tab) | 1.0 mg (mg/tab) |
|-------------------------------------|-----------------------|-----------------|-----------------|
| Drug substance (model) | 0.50 | 0.50 | 1.00 |
| Microcrystalline cellulose | 62.92 | 62.92 | 125.84 |
| Dibasic calcium phosphate anhydrous | 33.33 | 33.33 | 66.66 |
| Croscarmellose sodium | 2.00 | 2.00 | 4.00 |
| Colloidal silicon dioxide | 0.50 | 0.50 | 1.00 |
| Magnesium stearate | 0.50 | 0.50 | 1.00 |
| Magnesium stearate | 0.25 | 0.25 | 0.50 |
| TOTAL: | 100.00 | 100.00 | 200.00 |

HPLC Assay Method

Assay of bypass, sieve cut, granulation, and tablet samples was accomplished by high-pressure liquid chromatography (HPLC; Agilent Technologies, Palo Alto, CA). Isocratic HPLC on a Waters Symmetry C18 column (5 μ m particle size, 15 cm length \times 3.9 mm i.d.; Waters, Milford, MA) was used to analyze the solutions by using a mobile phase comprised of phosphoric acid (Fisher Chemicals, Fairlawn, NJ)/triethylamine (Burdick and Jackson, Muskegon, MI) (0.3%/0.2%, v/v): methanol (90:10, v/v), a column temperature of 35°C, an elution time of approximately 5 min and UV detection.

Processing Methods

To understand the effect of the roller compaction and milling parameters on the drug content uniformity in the granulation, first the effect of two roller compaction parameters, namely, roll force (RF) and average gap width (GW), was investigated by measuring bypass weight % and bypass potency (Study I). Afterward, two milling parameters, namely, granulating sieve size (SS) and granulator speed (GS), were included in a D-optimal response surface design (Study II) along with RF and GW. Finally, the impact of the optimized roller compaction and milling conditions on granulation and tablet content uniformity was determined through the manufacture and evaluation of a confirmation trial batch.

A 150-kg scale batch was manufactured and processed as 33 subbatches for execution of a two-part design of experiments (DOE) that investigated the effects of the four roller compaction/milling process parameters. The excipients were added to a 400-L bin (J. Engelsmann AG, Westheim, Germany) and blended for 30 min at 12 rpm. The blend was then passed through a mill (Quadro Comil 197S, Millburn, NJ) fitted with a 0.8-mm sieve as a delumping step, and lubricant was then added to the bin and blended for 2 min at 12 rpm.

After lubrication, the bin was docked above a 3-W Polygran 250/100/3 roller compactor, shown in Figure 1 (Gerteis Maschinen + Processengineering AG, Jona, Switzerland). The blend was roller compacted in 2- to 3-kg subbatches according to a two-part DOE. For Study I, the milling apparatus (rotor and sieve) was removed from the Gerteis so that ribbons and bypass could be collected to measure bypass weight % through the rolls and bypass potency, as well as to evaluate ribbon quality. Ribbons were collected only after the target roll force and gap width had been achieved. Ten runs were performed according to the DOE in Table 2 with RF and GW as the independent variables. Roll speed was maintained at 10 rpm for all runs.

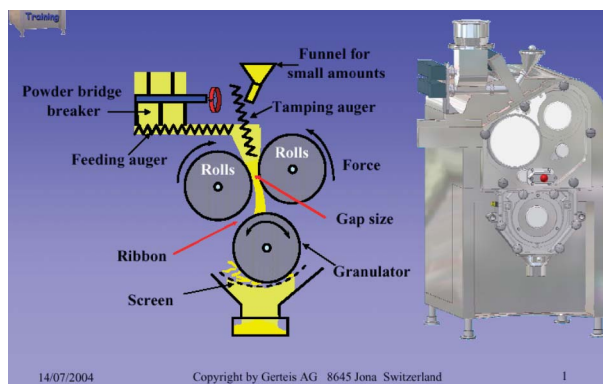


Figure 1. Schematic of the Gerteis 3-W Polygran Roller Compactor Courtesy of Gerteis Maschinen + Processengineering AG (Jona, Switzerland).

For Study II the milling apparatus (i.e., granulator) was reinstalled on the roller compactor, and four process variables were studied (Table 3): RF, GW, SS, and GS. The roll speed was held constant at 10 rpm, and granulator oscillating mill angle was set clockwise for 150° and counterclockwise for 210°. Twenty-three runs were performed for Study II. A lubricant was added to the granulation and blended in a 10-L bin (L.B. Bohle Inc., Bristol, PA) for 3 min. The lubed granulations were tested for particle size, sieve cut potency, granulation potency, and uniformity.

Each granulation from Study II of the DOE was compressed at 60,000 tablets per hour on a T-100 rotary tablet press (Kilian & Co. Inc., Horsham, PA). Tablets were compressed to a weight of 100 mg. The 100-mg tablets were made by using nine stations of 7/32-inch standard round concave tooling. A five-point crushing strength-compression profile was created for each subbatch at 2, 4, 6, 8, and 10 kN compression force. For each compression force, 20 tablets were evaluated for weight, crushing strength, and friability. After completing the crushing strength-compression profiles, the remaining granulation was tableted, and samples were collected for tablet potency and uniformity analysis.

Bypass Properties (Study I)

Bypass Weight %, Bypass Potency

During the granulation step of Study I, the Gerteis in-line mill (rotor and sieve) was removed. Ribbons were collected on a 1-mm sieve at the compactor discharge, while the bypass was transferred through the sieve into a polyethylene (PE) bag. The bypass weight % was measured for each run, and the potency of the bypass was determined via the HPLC assay method.

Table 2

Target and Experimental Values for Process Parameters in Study I of the Roller Compaction DOE using a 3² Full Factorial Design on RF and GW and Associated Response Values

| Run Order | Roll Force (kN) | | Gap Width (mm) | | % Bypass (Weight %) | Bypass Potency (% of Intent) |
|-----------|-----------------|--------|----------------|--------|---------------------|------------------------------|
| | Target | Actual | Target | Actual | | |
| 1 | 4 | 4 | 3.5 | 3.50 | 12.5 | 93.2 |
| 2 | 12 | 12 | 3.5 | 3.35 | 0.8 | 87.8 |
| 3 | 12 | 12 | 1.7 | 1.40 | 1.4 | 91.6 |
| 4 | 8 | 8 | 1.7 | 1.50 | 1.6 | 88.8 |
| 5 | 4 | 4 | 2.6 | 2.60 | 3.7 | 89.8 |
| 6 | 8 | 8 | 2.6 | 2.60 | 3.3 | 94.4 |
| 7 | 4 | 4 | 1.7 | 1.70 | 1.0 | 86.2 |
| 8 | 12 | 12 | 2.6 | 2.60 | 1.0 | 88.0 |
| 9 | 8 | 8 | 3.5 | 3.50 | 1.5 | 88.6 |
| 10 | 4 | 4 | 3.5 | 3.40 | 16.6 | 95.2 |

Table 3

Target and Experimental Values for Process Parameters in Study II of the Roller Compaction DOE Using a D-Optimal Response Surface Design

| Run Order | Roll Force (kN) | | Gap Width (mm) | | Sieve Size (mm) | Granulator Speed (rpm) |
|-----------|-----------------|--------|----------------|--------|-----------------|------------------------|
| | Target | Actual | Target | Actual | | |
| 1 | 12 | 12 | 1.7 | 1.80 | 0.8 | 100 |
| 2 | 4 | 4 | 3.5 | 3.45 | 0.8 | 100 |
| 3 | 12 | 12 | 3.5 | 3.35 | 0.8 | 25 |
| 4 | 4 | 4 | 1.7 | 1.65 | 0.8 | 25 |
| 5 | 12 | 12 | 3.5 | 3.25 | 0.8 | 100 |
| 6 | 4 | 4 | 3.5 | 3.45 | 1.5 | 25 |
| 7 | 4 | 4 | 1.7 | 1.65 | 1.5 | 100 |
| 8 | 12 | 12 | 1.7 | 1.50 | 1.5 | 25 |
| 9 | 12 | 12 | 3.5 | 3.25 | 1.5 | 100 |
| 10 | 12 | 12 | 3.5 | 3.25 | 1.0 | 25 |
| 11 | 8 | 8 | 2.6 | 2.45 | 1.0 | 50 |
| 12 | 4 | 4 | 3.5 | 3.40 | 1.0 | 100 |
| 13 | 8 | 8 | 3.5 | 3.35 | 1.5 | 100 |
| 14 | 12 | 12 | 3.5 | 3.20 | 1.5 | 50 |
| 15 | 12 | 12 | 1.7 | 1.50 | 1.5 | 100 |
| 16 | 4 | 4 | 1.7 | 1.63 | 1.5 | 25 |
| 17 | 12 | 12 | 2.6 | 2.45 | 1.5 | 25 |
| 18 | 12 | 12 | 1.7 | 1.45 | 0.8 | 25 |
| 19 | 4 | 4 | 3.5 | 3.45 | 0.8 | 50 |
| 20 | 8 | 8 | 3.5 | 3.30 | 0.8 | 25 |
| 21 | 4 | 4 | 1.7 | 1.65 | 0.8 | 100 |
| 22 | 4 | 4 | 2.6 | 2.52 | 0.8 | 25 |
| 23 | 12 | 12 | 1.7 | 1.40 | 0.8 | 100 |

Granulation Properties (Study II)

Particle Size

Granulation particle size was measured for each granulating condition by using sieve analysis. The sieve

analysis was carried out to determine the geometric mean granule size. Approximately 5 g of granule sample was transferred to the top of a stacked set of seven preweighed sieves of decreasing size: 840, 425, 250, 180, 150, 75, and 45 μ m. The sieves were shaken for 7.5 min with an amplitude of 6 and pulse setting of 6 on a Model L3 Sonic Sifter

(Allen-Bradley, Milwaukee, WI). These conditions were previously determined to cause no detrimental effect on the particle size distribution due to the test method and procedure. The sieves were then disassembled and reweighed to determine the weight fraction of granules retained on each sieve. These weights were converted to mass percentage. The geometric mean granule size was calculated from these mass fractions according to the method described by Lantz et al.^[19]

Sieve Cut Uniformity

The sieve cuts collected from each granulation were analyzed for potency using the HPLC method. Individual sieve cut samples, ranging from 0.5 to 2 g, were analyzed in their entirety allowing for a more accurate assessment of the amount of drug present in each sieve cut sample. To achieve a consistent target sample concentration for analysis, within the validated range of the HPLC method, each sample was prepared in sufficient volume to achieve a concentration of approximately 0.01 mg drug/mL. This was accomplished by taking into account the sample weight and theoretical ratio of drug to granulation amount. The variability in drug potency as a function of particle size was assessed by calculating the percent relative standard deviation (%RSD) of the sieve cut potency samples for each run.

Granulation Potency and Uniformity

Granulation potency and uniformity were assessed on six 2-g samples removed from each granulation after lubrication. Three sampling locations from two zones of the bin (top and bottom) were used. Samples were removed directly from the bin by using an open face thief and analyzed via the HPLC assay method. The mean and standard deviation of granulation potency were calculated.

Segregation Testing

The potentials for sifting and fluidization segregation of the original and optimized granulations were measured by Jenike & Johanson, Inc. according to the published ASTM methods.^[20,21] During fluidization segregation potential testing, a powder sample was fluidized for a period of time within a chamber and then allowed to come to rest. Samples from the top, center, and bottom of the chamber were then analyzed for potency. The greater the difference in potency values among samples, the greater the potential for the powder to segregate via a fluidization mechanism.

When testing for sifting segregation potential, a powder sample was passed through a steep cone hopper into a shallow cone hopper. The contents were then allowed to

flow out of the shallow hopper through a discharge chute. Samples were collected at the beginning, middle, and end of the discharge process. The greater the difference in potency values among samples, the greater the potential for the powder to segregate via a sifting mechanism.

Tablet Properties (Study II)

Compression Force at Target Crushing Strength

Tablet crushing strength was measured by using a Model 6D tablet tester (Schulinger Pharmatron, Manchester, NH). Each of the 23 runs in Study II was tableted at five different compression forces. For each compression force, the crushing strength of 20 tablets was measured, and the average was calculated. The compression force required to produce a tablet of the target crushing strength (7 kP) was determined from a plot of tablet crushing strength versus compression force.

Friability

Tablets from each of the five compression forces for every run in Study II were tested for friability by tumbling 20 tablets in a VanKel Friabilator (VanKel Industries Inc., Cary, NC) for 4 min at 25 rpm.

Stratified Tablet Potency and Uniformity

Tablets were collected at five evenly spaced time points throughout each tableting run in Study II. For each time point, five tablets were analyzed by the HPLC assay method to assess the potency (mean) and uniformity (% RSD) of each run.

Statistical Analysis

Study I consisted of two independent variables, RF and GW, each at three levels (i.e., a 3² full factorial design), with two responses that were analyzed statistically: bypass weight % and bypass potency. Main effects and significant interaction terms were modeled by using multiple-regression analysis techniques. The regression model for the two independent variables in Study I can be represented by the following general form:

$$Y_I = \alpha_0 + \alpha_1 \text{ RF} + \alpha_2 \text{ GW} + \alpha_3 \text{ RF*GW} + \alpha_4 \text{ RF}^2 + \alpha_5 \text{ GW}^2 \quad (1)$$

where $\alpha_0, \alpha_1, \dots, \alpha_i, \dots, \alpha_5$ for $i = 0$ to 5 are the coefficients of the model.

Study II contained four independent variables (RF, GW, SS, and GS) in a D-optimal response surface design.^[22] The eight critical responses investigated were mean granulation particle size, sieve cut potency uniformity, mean granulation potency, granulation uniformity, tablet potency, tablet uniformity, compression force to achieve target crushing strength (7 kP), and friability at target crushing strength (7 kP). To aid the statistical analysis, the independent variable values were transformed into coded values using mathematical equations. Main effects, interactions effects, and quadratic effects were calculated for the four independent variables in Study II, as represented in the general equation below:

$$Y_{II} = \beta_0 + \beta_1 \text{RF} + \beta_2 \text{GW} + \beta_3 \text{SS} + \beta_4 \text{GS} \\ + \beta_5 \text{RF*GW} + \beta_6 \text{RF*SS} + \beta_7 \text{RF*GS} \\ + \beta_8 \text{GW*SS} + \beta_9 \text{GW*GS} + \beta_{10} \text{SS*GS} \\ + \beta_{11} \text{RF}^2 + \beta_{12} \text{GW}^2 + \beta_{13} \text{SS}^2 + \beta_{14} \text{GS}^2 \quad (2)$$

where $\beta_0, \beta_1, \dots, \beta_i, \dots, \beta_{14}$ for $i = 0$ to 14 are the coefficients of the model.

An important objective of the statistical analysis was to derive parsimonious models that would be able to predict the results of future experiments with adequate reliability. To achieve this goal, the primary tool used to construct the predictive models was maximization of R^2 for prediction (which is equivalent to minimization of the PRESS statistic). Joint statistical significance of all the terms in the model (i.e., the “overall” or “model” p -value) and the statistical significance of the individual terms in the model (i.e., the individual p -values) were also considered during model selection. Individual p -values were reliable statistics due to the minimal degree of collinearity achieved by the D-optimal statistical design. In all cases, the Effect Hierarchy Principle was applied: that is, if a two-way interaction were deemed statistically significant, then the two main effects were also included in the predictive model.^[23] Likewise, if a quadratic term were deemed statistically significant, then the corresponding main effect was also included in the model.

RESULTS AND DISCUSSION

The critical response values for each run of Study I and Study II are shown in Tables 2 and 4, respectively. The statistical analyses for Studies I and II are presented in Table 5. The target roll force was achieved directly following start-up at the new set point. The target gap width

was not achieved in every run, and therefore the actual average was recorded in Tables 2 and 3.

Study I Results: Bypass Properties

Bypass Weight % and Bypass Potency

Table 5 gives the regression coefficient and associated p -value for each individual term in each predictive model from Study I. In addition, each model's overall p -value and R^2 for prediction are provided. The regression model for bypass weight % provides evidence of a strong interaction between RF and GW ($p = 0.0046$). Overall, the model had an acceptably high R^2 for prediction (0.6809), with good evidence of statistical significance ($p = 0.0022$). The regression model for bypass potency had a low R^2 for prediction (0.3649), and its statistical significance was marginal ($p = 0.0868$). The final regression models describing the bypass properties of Study I are listed in Equations (3–4).

$$\text{Ln[Bypass Wt\%]} = 0.70 - 0.71\text{RF} \\ + 0.37 \text{GW} - 0.81 \text{RF*GW} \quad (3)$$

$$\text{Bypass Potency} = 89.9 - 0.7 \text{RF} \\ + 0.8 \text{GW} - 2.9 \text{RF*GW} \quad (4)$$

The contour plot for bypass weight %, shown in Figure 2, indicates greater bypass when RF was below 8 kN and GW was above 2.6 mm. This region of the contour plot for bypass weight % reflects what would be expected from suboptimal roller compaction parameters at a constant feed rate, namely, bypass weight % increased when roll force decreased and/or gap width increased.

It was observed that ribbon splitting had occurred during runs 2, 8, and 9 [i.e., the (high, high), (high, mid), and (mid, high) combinations of RF and GW], where the RF was too great for the GW being used. Combining this observation with the bypass data, it was clear that to avoid both bypass and ribbon quality issues, the optimum GW should be below 2.6 mm.

Gap width was measured several times throughout the run, and the average was used in the statistical analysis. Runs 1 and 10 were not true replicates when using the actual average value during manufacture of that portion of the batch. Therefore, no lack-of-fit test could be performed. However, the data were analyzed for lack-of-fit using the average gap width for Runs 1 and 10 at 3.45 mm. The p -values for lack-of-fit were not statistically significant (0.6396 for bypass weight percent and 0.4270 for bypass potency).

Table 4
Response Values from Study II

| Run Order | Mean Granulation Particle Size (μm) | Sieve Cut Uniformity (%RSD of Sieve Cut Potency) | Mean Granulation Potency (% Intent) | Granulation Uniformity (%RSD of Potency) | Mean Tablet Potency (% Intent) | Tablet Uniformity (%RSD of Potency) | Compression Force at 7kP Crushing Strength (kN) | Friability at 7kP Crushing Strength (%) |
|-----------|-------------------------------------|--|-------------------------------------|--|--------------------------------|-------------------------------------|---|---|
| II-1 | 145.6 | 13.0 | 99.2 | 0.6 | 99.2 | 0.6 | 9.7 | 0.03 |
| II-2 | 136.8 | 34.4 | 98.4 | 0.7 | 97.5 | 0.8 | 4.8 | 0.14 |
| II-3 | 171.6 | 19.5 | 99.3 | 0.5 | 98.9 | 0.5 | 8.3 | 0.05 |
| II-4 | 144.4 | 28.9 | 98.6 | 0.7 | 98.2 | 0.8 | 5.1 | 0.03 |
| II-5 | 170.8 | 14.5 | 99.4 | 0.5 | 98.7 | 0.3 | 8.0 | 0.15 |
| II-6 | 147.5 | 35.8 | 98.2 | 0.6 | 97.5 | 0.7 | 4.5 | 0.03 |
| II-7 | 211.9 | 27.5 | 97.8 | 0.8 | 97.6 | 1.5 | 5.1 | 0.18 |
| II-8 | 474.5 | 28.1 | 99.3 | 0.8 | 98.9 | 1.0 | 11.0 | 0.07 |
| II-9 | 401.6 | 22.9 | 98.1 | 5.1 | 99.0 | 0.5 | 7.7 | 0.14 |
| II-10 | 166.9 | 36.6 | 97.5 | 2.6 | 98.5 | 0.5 | 8.1 | 0.03 |
| II-11 | 159.4 | 31.6 | 97.8 | 0.4 | 98.7 | 0.8 | 6.7 | 0.04 |
| II-12 | 133.0 | 44.6 | 97.0 | 0.2 | 97.7 | 0.7 | 4.5 | 0.07 |
| II-13 | 320.6 | 20.0 | 97.0 | 1.2 | 97.9 | 0.8 | 6.7 | 0.05 |
| II-14 | 326.6 | 16.7 | 98.2 | 2.0 | 98.5 | 1.0 | 7.8 | 0.03 |
| II-15 | 345.9 | 12.8 | 97.8 | 1.7 | 98.7 | 0.6 | 9.5 | 0.03 |
| II-16 | 215.4 | 29.4 | 96.4 | 1.3 | 96.8 | 0.8 | 4.4 | 0.02 |
| II-17 | 317.1 | 16.0 | 97.1 | 1.5 | 98.1 | 0.6 | 8.1 | 0.10 |
| II-18 | 176.6 | 12.5 | 98.3 | 0.7 | 98.7 | 0.6 | 10.5 | 0.00 |
| II-19 | 128.6 | 34.7 | 98.2 | 0.9 | 97.8 | 0.6 | 4.7 | 0.01 |
| II-20 | 150.9 | 21.8 | 99.1 | 0.7 | 98.4 | 0.7 | 6.3 | 0.03 |
| II-21 | 139.1 | 25.9 | 97.5 | 0.5 | 97.3 | 0.8 | 5.3 | 0.02 |
| II-22 | 143.6 | 25.3 | 98.2 | 0.5 | 96.8 | 0.8 | 4.9 | 0.00 |
| II-23 | 190.3 | 14.6 | 98.9 | 0.4 | 97.8 | 0.6 | 9.8 | 0.03 |

Study II Results: Granulation Properties

Mean Granulation Particle Size

A strong interaction ($p = 0.0006$) between RF and SS was seen in the mean particle size contour plot (Figure 3). As SS became smaller, RF had a decreased effect on granulation particle size. The regression model predicts that a 0.8-mm SS should produce granulations with average particle sizes between 135 and 165 μm, a 1.0-mm SS should produce granulations with average particle sizes between 150 and 220 μm, and a 1.5-mm SS should produce granulations with average particle sizes between 195 and 375 μm. The final regression model describing the mean granulation particle size for Study II (Table 5) is listed in Equation (5).

$$\text{Mean Granulation PS} = 216 + 51 \text{ RF} + 68 \text{ SS} + 38 \text{ RF*SS} \quad (5)$$

Actual response values for the mean granulation particle size ranged from 129 to 475 μm, whereas predicted

response values ranged from 134 to 373 μm. The model cannot reliably predict mean particle size for SS above 1.5 mm and RF above 12 kN. The R^2 for prediction (0.8069), the overall p -value (< 0.0001), and the randomized run order of experimental conditions provided very strong evidence of cause and effect.

Sieve Cut Uniformity

RF had a significant linear effect ($p < 0.0001$) on the granulation sieve cut uniformity (Figure 4). SS had a quadratic effect on the granulation sieve cut uniformity ($p < 0.0001$). R^2 for prediction (0.6521) was also strong. The actual response values listed in Table 4 range from 12.5 to 44.6% and closely match the predicted response values shown in Figure 4 of 15.9 to 44.0%. The model shows that the granulation sieve cut uniformity was worst with the 1.0 mm sieve. The actual values (Table 4) ranged from 12.5 to 34.7% for the 0.8-mm sieve, from 31.6 to 44.6% for the 1.0-mm sieve, and from 12.8 to 35.8% for the 1.5-mm sieve.

Sieve size affected mean granulation particle size, mean granulation potency, and tablet content uniformity,

Table 5
Intercepts, Regression Coefficients, and p-values for Coded Predictive Models from Study I and II

| Response (intercept) | RF Coefficient (p-value) | GW Coefficient (p-value) | SS Coefficient (p-value) | GS Coefficient (p-value) | RF *GW Coefficient (p-value) | RF*SS Coefficient (p-value) | SS ² Coefficient (p-value) | Overall p-value | R ² for Prediction |
|---------------------------------------|--------------------------|--------------------------|--------------------------|--------------------------|------------------------------|-----------------------------|---------------------------------------|-----------------|-------------------------------|
| Study I | | | | | | | | | |
| Ln Bypass Wt % (0.70) | -0.71 (0.0045) | 0.37 (0.0479) | n.a. | n.a. | -0.81 (0.0046) | n.a. | n.a. | 0.0022 | 0.6809 |
| Bypass Potency (89.9) | -0.7 (0.4488) | 0.8 (0.3962) | n.a. | n.a. | -2.9 (0.0276) | n.a. | n.a. | 0.0868 | 0.3649 |
| Study II | | | | | | | | | |
| Mean Gran Particle Size (216) | 51 (<0.0001) | — | 68 (<0.0001) | — | — | 38 (0.0006) | — | <0.0001 | 0.8069 |
| Sieve Cut RSD (41.4) | -6.4 (<0.0001) | — | 1.2 (0.2650) | — | — | — | -17.9 (<0.0001) | <0.0001 | 0.6521 |
| Mean Gran Potency (97.0) | 0.4 (0.0130) | — | -0.5 (0.0022) | — | — | — | 1.2 (0.0215) | 0.0015 | 0.3543 |
| Log(Gran RSD) (-0.07) | 0.10 (0.0758) | — | 0.17 (0.0051) | — | — | — | — | 0.0038 | 0.2555 |
| Mean Tablet Potency (98.1) | 0.6 (<0.0001) | — | — | — | — | — | — | <0.0001 | 0.5878 |
| Log(Tablet Potency RSD) (-0.15) | -0.08 (0.0025) | -0.06 (0.0308) | 0.06 (0.0180) | — | — | — | — | 0.0020 | 0.2920 |
| CF@Crushing Strength=7kP (6.8) | 2.0 (<0.0001) | -0.6 (<0.0001) | — | — | -0.5 (0.0002) | — | — | <0.0001 | 0.9502 |
| Friab@ Crushing Strength = 7kP (0.06) | — | — | — | 0.02 (0.0320) | — | — | — | 0.0320 | 0.0340 |

n.a. means not applicable for Study I which removed the granulator system.

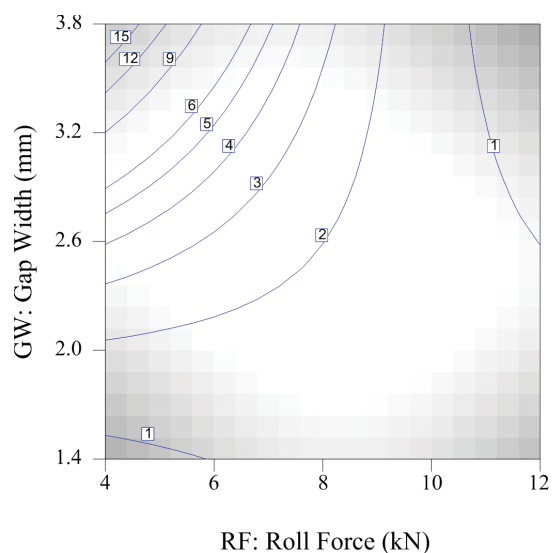


Figure 2. Contour Plot for Study I (numerical values listed on contours represent the bypass weight %).

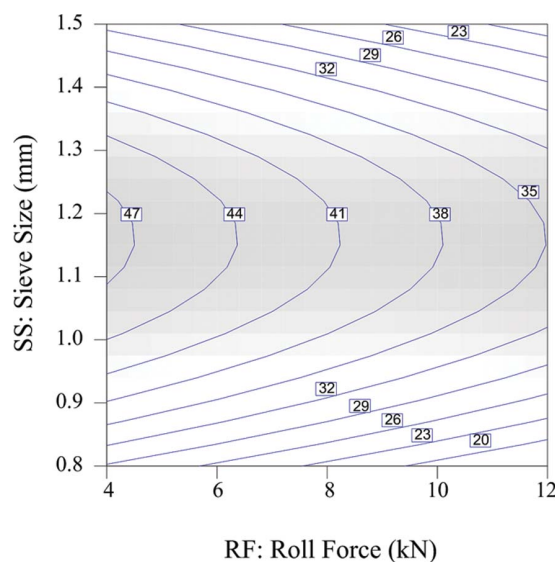


Figure 4. Contour Plot for Granulation Sieve Cut % RSD from Study II.

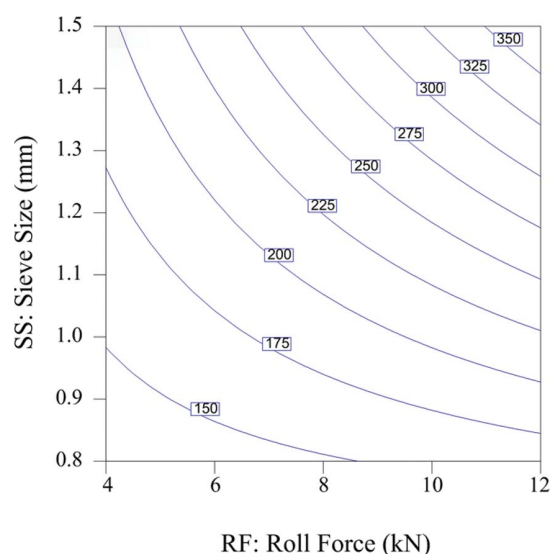


Figure 3. Contour Plot for Mean Granulation Particle Size (microns) from Study II.

so it is not surprising that it affected sieve cut uniformity. However, there was no statistically significant linear effect for sieve size on sieve cut uniformity, even if only the data using the 0.8-mm and 1.5-mm screens were modeled. So, there was either no sieve size effect on sieve cut uniformity or the effect was quadratic.

It is true that the 1.0-mm screen (which was the source of the quadratic effect for sieve size) was set up just once, whereas the 0.8-mm screen and the 1.5-mm screen were both set up twice. However, if there was a problem

with the installation of the 1.0-mm screen, then it would have had to affect only sieve cut uniformity and mean granulation potency, because no statistically significant quadratic effect for sieve size was detected for any other response.

Because of the lack of appreciable collinearity in the experimental design, the inclusion of the quadratic effect in the predictive model for sieve cut uniformity did not affect the magnitude of the estimate for the roll force effect. Because neither of the other two response constraints that defined the optimum roller compaction region was affected by sieve size, the optimization plot still serves as the operating region at any screen size.

The final regression model describing the potency uniformity as a function of granulation particle size for Study II is listed in Equation (6).

$$\begin{aligned} \text{Sieve Cut Potency Uniformity} = & 41.4 + 1.2 \text{ SS} \\ & - 6.4 \text{ RF} - 17.9 \text{ SS}^2 \quad (6) \end{aligned}$$

Mean Granulation Potency and Uniformity

RF and SS had slight effects on granulation potency. The overall p -value (0.0015) was significant, but the R^2 for prediction (0.3543) was not strong. The predicted response values ranged from 97.1 to 99.0% and the actual response values ranged from 96.4 to 99.4%. Based on the trend seen, it can be inferred that 0.8-mm SS will give higher potencies as opposed to the other two SS. The

higher granulation potency values suggest improved incorporation of drug into the granulation, which translates to less segregation during subsequent processing by reduction of the superpotent ungranulated material.

RF and SS may have had statistically significant effects (overall $p = 0.0038$) on granulation potency variability; however the reliability of the model (R^2 for prediction = 0.2555) is not sufficient to predict results of future runs. The model predicted response values from 0.45 to 1.58% but could not predict some of the larger variabilities. The actual response values ranged from 0.2 to 5.1%. The utility of this model is deemed higher than might otherwise be expected with weak values for model predictability and significance, because the same two parameters were in this predictive model as were in the granulation potency model. The model illustrates a trend: as the screen size increased, the granulation potency variability, represented by the %RSD, also increased.

Study II Results: Tablet Properties

Stratified Tablet Potency and Uniformity

RF had a strong effect on stratified tablet potency ($p < 0.0001$). An increase in RF correlated to increased tablet potency. Actual response values for stratified tablet potency ranged from 96.8 to 99.2% (Table 4). As discussed previously, higher potency values translate to less segregation during subsequent processing by reduction of the superpotent ungranulated material.

The final regression model describing the tablet potency for Study II is listed in Equation (7).

$$\text{Mean Tablet Potency} = 98.1 + 0.6 \text{ RF} \quad (7)$$

RF appeared to have an effect on tablet content uniformity ($p = 0.0025$). There was an indication that two other process variables, GW ($p = 0.0308$) and SS ($p = 0.0180$), affected tablet content uniformity, as well. The model indicates that smaller SS, higher RF, or larger GW improved tablet content uniformity independently of each other. Actual response values for the % RSD of the stratified tablet potency ranged from 0.3 to 1.5%.

Compression Force at Target Crushing Strength

RF and GW interacted strongly ($p = 0.0002$) to affect the compression force required to achieve the target tablet crushing strength of 7 kP. Decreasing RF significantly decreased the force needed during compression, especially at low GW. However, increasing GW significantly decreased the force needed during compression at high RF

only. Actual response values for the required compression force ranged from 4.4 to 11.0 kN. The contour plot (Figure 5) illustrates a very strong predictive model for this response variable (R^2 for prediction = 0.9502).

The final regression model for the tablet compression force of Study II is listed in Equation (8).

$$\begin{aligned} \text{Compression Force} = & 6.8 + 2.0 \text{ RF} \\ & - 0.6 \text{ GW} - 0.5 \text{ RF} \cdot \text{GW} \quad (8) \end{aligned}$$

Friability

Tablet friability at the target tablet crushing strength ranged from 0.00 to 0.18% for the 23 runs in Study II. None of the four roller compaction and milling parameters evaluated had an important effect on friability at a tablet crushing strength value of 7 kP. The regression model summarized in Table 5 had no meaningful predictive ability (R^2 for prediction = 0.0340).

Study I and II: Optimization

Before the statistical analysis was performed, constraints were placed on each response variable. The optimum combination of the four process parameters was expected to satisfy all these constraints simultaneously, with a robust operating region surrounding this optimum condition.

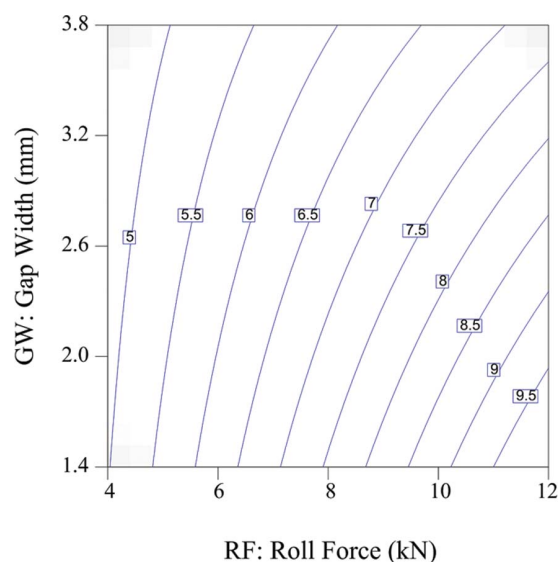


Figure 5. Contour Plot for Compression Force (kN) at Target Crushing Strength from Study II.

An overlay plot for Study I (Figure 6) was created by using the following constraints: predicted bypass weight % below 3.0%, and predicted bypass potency between the limits of 85.0 and 115.0%. The yellow region in this figure indicates the area simultaneously satisfying all constraints that had been placed on both bypass responses.

The constraint for granulation particle size was 125–175 μm . The constraint imposed on the granulation sieve cut potency was that the variability must be less than 22.5%. A constraint for acceptable mean granulation potency between 96.0 and 104.0% was applied. The upper limit for granulation variability was set at 1.0%.

The constraints placed on the tablet properties limited acceptable stratified tablet potency to 97.0–103.0%, with a % RSD below 1.0%. The suggested maximum acceptable compression force to reach the target tablet crushing strength was 8.5 kN. All conditions tested in Study II resulted in tablet friability within the applied limits of 0.0–0.2%.

To obtain an optimum region with $\text{GW} < 2.6 \text{ mm}$ (i.e., bypass weight % within constraints and no ribbon splitting), an overlay optimization plot (Figure 7) was created. It was clear from the statistical analysis of Study II that 0.8 mm was the optimum screen size. Because granulating speed had no meaningful effect on any response variable, $\text{GS} = 50 \text{ rpm}$ was selected as a robust setting. The yellow region in Figure 7 met all required criteria for the responses in Studies I and II when $\text{SS} = 0.8 \text{ mm}$ and $\text{GS} = 50 \text{ rpm}$. The proposed operating conditions ($\text{RF} = 9 \text{ kN}$, $\text{GW} = 2.3 \text{ mm}$, $\text{SS} = 0.8 \text{ mm}$, and $\text{GS} = 50 \text{ rpm}$) were selected at the center of the operating region to ensure process robustness. Note that the boundaries of this operating

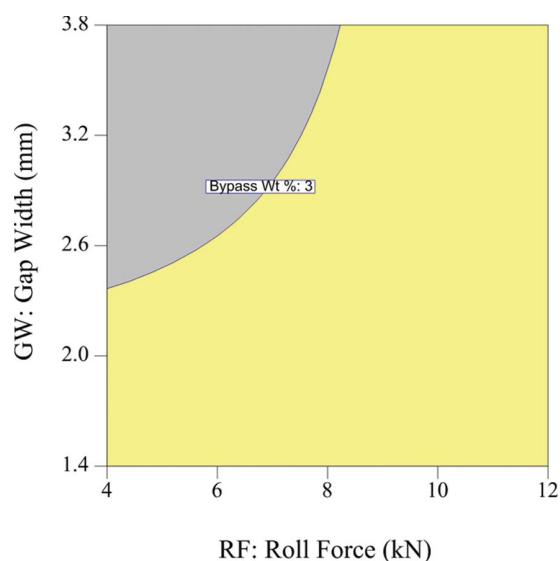


Figure 6. Overlay Plot for Study I Bypass Weight % and Bypass Potency.

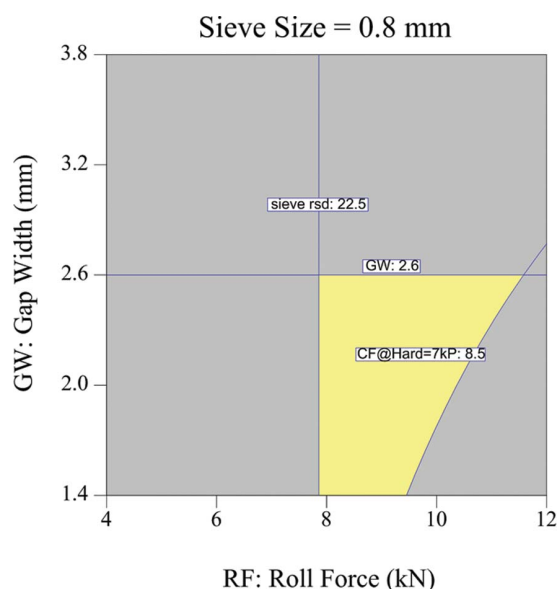


Figure 7. Overlay Optimization Plot Summarizing Constraints from Both Study I and II.

region were defined by one equipment constraint ($\text{GW} > 1.4 \text{ mm}$), one bypass-and-ribbon-quality constraint ($\text{GW} < 2.6 \text{ mm}$), one granulation constraint (sieve cut uniformity $< 22.5\%$), and one tableting constraint (compression force $< 8.5 \text{ kN}$ at target crushing strength).

Confirmation Trial

The reliability of the predictive models obtained from the statistical analyses of Studies I and II was evaluated by means of a 150-kg confirmation trial, using the four optimized processing parameters: $\text{RF} = 9 \text{ kN}$, $\text{GW} = 2.3 \text{ mm}$, $\text{SS} = 0.8 \text{ mm}$, and $\text{GS} = 50 \text{ rpm}$. Sieve cut uniformity, segregation potentials (sifting and fluidization), and stratified tablet potency uniformity of the confirmation batch were compared to the results from a preoptimized (hereinafter referred to as “original”) batch. The blend from the original batch was roller compacted on the Gerteis roller compactor by using the original processing parameters: $\text{RF} = 5 \text{ kN}$, $\text{GW} = 3.5 \text{ mm}$, $\text{SS} = 0.8 \text{ mm}$, and $\text{GS} = 50 \text{ rpm}$. Both the confirmation and original batches used the same formulation and processing and were prepared by using a bin blender, a Co-mil, and tableted to 100-mg weight (0.5-mg active tablet) using a Fette PT1200 rotary press (Fette Compacting, Schwarzenbek, Germany). Tableting of the confirmation batch was performed by using the same equipment; however, the first 75 kg of granulation were tableted to 100-mg weight, whereas the remainder of the granulation was tableted to 200-mg weight (1.0-mg active

tablet). This sequence of tablet manufacturing allowed a direct comparison between the stratified tablet potency uniformity of the 0.5-mg tablets made in the confirmation trial and the 0.5-mg tablets made during the initial 750,000 units of the original batch.

Segregation Testing

Results for the fluidization and sifting segregation testing on the final blend, for the original and confirmation batches, can be seen in Table 6. For the fluidization segregation testing, potency for the confirmation batch across top, center, and bottom was much more evenly distributed (92.3–104.4%) than the original batch where the potency ranged from 90.7 to 65.6% from top to bottom. Similarly, during sifting segregation testing, the potency across beginning, middle, and end samples ranged from 97.6 to 101.6% for the confirmation batch, whereas the potency dropped from 92.6 to 70.5% for the original batch.

Based on the above results, the segregation potential for the granulation produced in the confirmation batch due to a fluidization mechanism was rated in the “moderate” category. The potential to segregate due to a sifting mechanism for the confirmation batch granulation was rated as ‘low’ after implementing the optimum dry granulation conditions. The original batch was categorized as having a “high” potential for segregation due to both mechanisms. The optimized roller compaction parameters clearly lowered the segregation potential for the final blend.

Sieve Cut Potency

Results of the sieve cut potency obtained from the confirmation and original batches are illustrated in Figure 8 and tabulated in Table 7. The sieve cut potency variability was reduced significantly from 35.2 to 13.8% because of roller compaction process optimization.

Stratified Tablet Potency Uniformity

Stratified tablet potency uniformity for the first 750,000 tablets produced during the confirmation trial was compared to the first 750,000 tablets produced during the original batch (Figure 9), as described in Materials and Methods. Results from the statistical F-test performed on the two sets of data showed that the stratified tablet potency variability for the confirmation batch ($SD = 0.39$) was significantly lower ($p = 0.0016$) than the stratified tablet potency variability for the original batch ($SD = 0.84$). This statistical result showed that the optimized roller compaction parameters, which had already been shown to reduce the segregation potential of the final blend, were able to improve the content uniformity of tablets.

CONCLUSIONS

Guided by the statistical analyses of results from Studies I and II, the following levels of four roller compaction/milling parameters were recommended as the optimum processing region: $RF = 9 \pm 1$ kN, $GW = 2.3 \pm 0.3$ mm, $SS = 0.8$ mm, and $GS = 50$ rpm. GS was set to 50 rpm to maximize robustness, because the range of 25–100 rpm did not have any important effect on any of the response variables. The most favorable SS was 0.8 mm because it was the optimum screen size for several responses. When the milling process is set up by using $SS = 0.8$ mm and $GS = 50$ rpm, then the proposed roller compaction operating conditions ($RF = 9$ kN, $GW = 2.3$ mm) were at the center of the region where all constraints from both Study I and Study II were satisfied simultaneously. This method for selecting process parameters was expected to produce the most favorable robustness characteristics while providing the highest probability of simultaneously satisfying all granulation and tablet constraints.

Table 6
Impact of the Original and Optimized Dry Granulation Process Parameters on Fluidization and Sifting Segregation of the Granulations

| Sample Location | Fluidization Segregation Test Results (% Intent) | | Sifting Segregation Test Results (% Intent) | |
|---------------------------|--|--------------------|---|--------------------|
| | Original Batch | Confirmation Batch | Original Batch | Confirmation Batch |
| Top or Beginning | 90.7 | 92.3 | 92.6 | 97.6 |
| Center or Middle | 88.9 | 97.4 | 91.6 | 98.3 |
| Bottom or End | 65.6 | 104.4 | 70.5 | 101.6 |
| Reference (G) | 98.2 | 98.6 | 98.2 | 98.6 |
| Potential for Segregation | HIGH | MODERATE | HIGH | LOW |

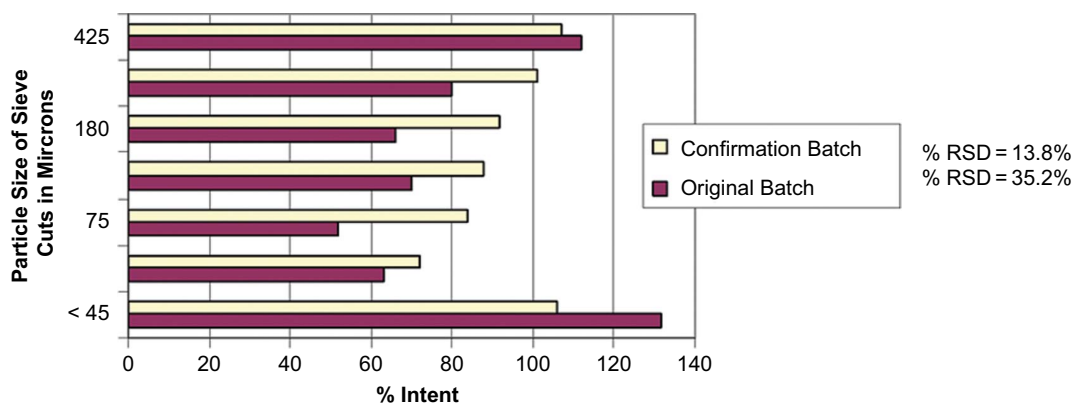


Figure 8. Comparison of the Sieve Cut Potency Values as a Function of Granule Particle Size (Confirmation vs. Original Batch).

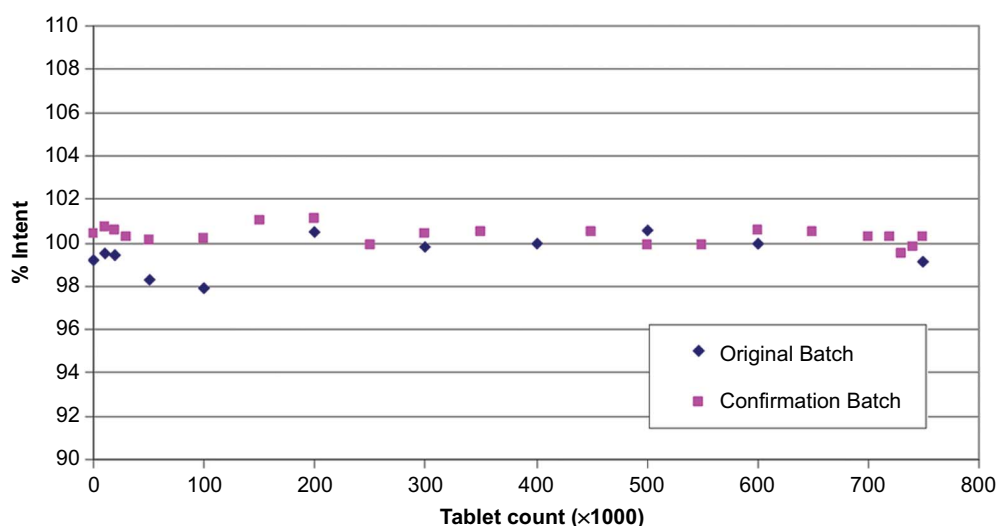


Figure 9. Comparison of the Stratified Tablet Potency (Confirmation vs. Original Batch).

Table 7
Sieve Cut Potency Test Results

| Sample Sieve Size (microns) | % Intent | |
|-----------------------------|----------------|--------------------|
| | Original Batch | Confirmation Batch |
| < 45 | 131.5 | 106.2 |
| 45 | 63.2 | 72.2 |
| 75 | 51.6 | 83.7 |
| 150 | 69.9 | 87.5 |
| 180 | 66.3 | 91.8 |
| 250 | 79.8 | 100.9 |
| 425 | 111.8 | 107.0 |
| % RSD | 35.2 | 13.8 |

On the basis of the results from the confirmation batch, it can be concluded that the optimization of the roller compaction parameters led to a more uniform distribution of granulation potency across granule particle size. This resulted in reduction of segregation potential for the final blend, as indicated by the segregation test results, and improved content uniformity of tablets, as shown by significantly decreased variability in stratified tablet potency data.

ACKNOWLEDGMENTS

The authors thank the following Pfizer colleagues for their contributions to this research: William Arikpo, Deborah Booth-Schindler, Bill Curatolo, Alanya Engrakul,

Bruno Hancock, Anja Kruse, Cynthia Oksanen, Kirsten Reinheimer, Yukun Ren, Daryl Simmons, Kim Vukovinsky, Carl Ziegler, and the TSC Operators (Sergio Capobianco, Ulrike Dufner, Marco Faller, Josef Hauser, Ioan Martinec, Jurgen Perin, Manfred Ringwald, Silvia Scheerer, Christian Weber, Frank Wick, Michael Widder). A special note of gratitude to Tom J. Baxter and James Prescott of Jenike & Johanson for their technical expertise in segregation and powder flow.

REFERENCES

- Hancock, B.C.; Colvin, J.T.; Mullarney, M.P.; Zinchuk, A.V. The relative densities of pharmaceutical powders, blends, dry granulations, and immediate-release tablets. *Pharm. Tech.* **2003**, 27 (4), 64–80.
- Prescott, J.K.; Hossfeld, R.J. Maintaining product uniformity and uninterrupted flow to direct-compression tableting presses. *Pharm. Technol.* **1994**, 18, 99–114.
- FDA Draft Guidance for Industry, Powder Blend and Finished Dosage Units—Stratified In-Process Dosage Unit Sampling and Assessment. October 2003.
- Kleinebudde, P. Roll compaction/dry granulation: Pharmaceutical applications. *Eur. J. Pharm and Biopharm.* **2004**, 58, 317–326.
- Shlieout, G.; Lammens, R.F.; Kleinebudde, P. Dry granulation with a roller compactor. I. The functional units and operation modes. *Pharm. Technol. Eur.* **2000**, 12 (11), 24–35.
- Shlieout, G.; Lammens, R.F.; Kleinebudde, P.; Bultman, M. Dry granulation with a roller compactor. II. Evaluating the operation modes. *Pharm. Technol. Eur.* **2002**, 14 (9), 32–39.
- Michoel, A.; Verlinden, W.; Rombaut, P.; Kinget, R.; De Smet, P. Carrier granulation: A new procedure for the production of low-dosage forms. *Pharm. Tech.* **1988**, 12 (6), 66–84.
- McKenna, A.; McCafferty, F. Effect of particle size on the compaction mechanism and tensile strength of tablets. *J. Pharm. Pharmacol.* **1982**, 34, 347–351.
- Malkowska, S.; Khan, K.A. Effect of re-compression on the properties of tablets prepared by dry granulation. *Drug Dev. Ind. Pharm.* **1983**, 9 (3), 331–347.
- Falzone, A.M.; Peck, G.E.; McCabe, G.P. Effects of changes in roller compactor parameters on granulations produced by compaction. *Drug Dev. Ind. Pharm.* **1992**, 18, 469–489.
- Kochhar, S.K.; Rubinstein, M.H.; Barnes, D. The effects of slugging and recompression on pharmaceutical excipients. *Int. J. Pharm.* **1995**, 115, 35–43.
- Inghelbrecht, S.; Remon, J.P.; Fernandes de Aguiar, P.; Walczak, B.; Massart, D.L.; Van De Velde, F.; De Baets, P.; Vermeersch, H.; De Backer, P. Instrumentation of a roll compactor and the evaluation of the parameter settings by neural networks. *Int. J. Pharm.* **1997**, 148, 103–115.
- Inghelbrecht, S.; Remon, J.P. Roller compaction and tableting of microcrystalline cellulose/drug mixtures. *Int. J. Pharm.* **1998**, 161, 215–224.
- Inghelbrecht, S.; Remon, J.P. The roller compaction of different types of lactose. *Int. J. Pharm.* **1998**, 166, 135–144.
- Rambali, B.; Baert, L.; Jans, E.; Massart, D.L. Influence of the roll compactor parameter settings and the compression pressure on the buccal bio-adhesive tablet properties. *Int. J. Pharm.* **2001**, 220, 129–140.
- von Eggelkraut-Gottanka, S.G.; Abu Abed, S.; Mueller, W.; Schmidt, P.C. Roller compaction and tableting of St. John's wort plant dry extract using a gap width and force controlled roller compactor. I. Granulation and tableting of eight different extract batches. *Pharm. Dev. Technol.* **2002**, 7, 433–445.
- von Eggelkraut-Gottanka, S.G.; Abu Abed, S.; Mueller, W.; Schmidt, P.C. Roller compaction and tableting of St. John's wort plant dry extract using a gap width and force controlled roller compactor. II. Study of roller compaction variables on granule and tablet properties by a 3^3 factorial design. *Pharm. Dev. Technol.* **2002**, 7, 447–455.
- Handbook of Pharmaceutical Excipients*, 4th Ed; Rowe, R.C.; Sheskey, P.J.; Weller, P.J., Eds. Chicago: Pharmaceutical Press, 2003.
- Lantz Jr., R.J. Size reduction. In *Pharmaceutical Dosage Forms: Tablets*, Vol. 2; Lieberman, H.A.; Lachman, L.; Schwartz, J.B., Eds. Marcel Dekker Inc.: New York, 181–187.
- Standard practice for measuring sifting segregation tendencies of bulk solids (D 6940-03). *Annual Book of ASTM Standards*, Vol 04.08, August 2003.
- Standard practice for measuring fluidization segregation tendencies of powders (D 6941-03). *Annual Book of ASTM Standards*, Vol 04.08, August 2003.
- Wald, A. On the efficient design of statistical investigations. *Ann. Math. Stat.* **1943**, 14, 134–140.
- Peixoto, J. L. A property of well-formulated polynomial regression models. *Am. Stat.* **1990**, 44 (1).